Coherent mapping helps identify abnormal potentials and improves the treatment of multiple ventricular tachycardia: A case report

Tadashi Hoshiyama, MD, PhD, Takumi Nagakura, MD, Hisanori Kanazawa, MD, PhD, Kenichi Tsujita, MD, PhD

From the Department of Cardiovascular Medicine, Graduate School of Medical Sciences, Kumamoto University, Kumamoto, Japan.

Introduction

As per current guidelines, radiofrequency catheter ablation (RFCA) is recommended for drug-refractory sustained ventricular tachycardia (VT), or VT storm, in the patients with scar-related heart disease.[1,2] Although RFCA decreases VT recurrence compared to medical therapy,[3] the recurrence rate still remains high, with values reported between 30% and 39%.[3,4] One of the mechanisms causing VT recurrence is the existence of multiple VT circuits owing to large scar areas.[5] In cases with large scar areas in the ventricle, it is difficult to differentiate which abnormal potentials are related to the critical VT circuit among the widely spread abnormal electrograms. Thus, RFCA for these multiple VTs remains challenging.

In this report, we present a case of a patient who had multiple VTs despite a previous RFCA for VT storm. Three-dimensional mapping using a coherent map integrated with a vector map (CARTO®3 version 7; Biosense Webster Inc, Diamond Bar, CA) helped to distinguish between critical targets in widely spread abnormal electrograms in the left ventricle (LV) and critical targets elsewhere, because the critical target is represented as slow conduction areas, and these slow conduction areas matched the critical VT circuit

confirmed by electrophysiological study. RFCA for these areas eradicated VT; furthermore, VT had not been induced following RFCA. A previous report has already shown that a coherent map integrated with a vector map may be useful, especially for complex supraventricular tachycardias.[6] Although this case was not a supraventricular tachycardia but a VT, this coherent map integrated with a vector map might unveil the critical abnormal potential among the widely spread multiple abnormal potentials.

A coherent map integrated with a vector map may be useful for scar-related VTs, especially those having multiple VT circuits.

Case report

A 67-year-old man was referred to our hospital for defibrillation treatment with an implantable cardioverter-defibrillator for VT. Coronary artery bypass grafting had been performed in this patient for myocardial infarction at 38 years of age. Cardiac resynchronization therapy, defibrillator implantation, and mitral valve replacement had been performed for left ventricular dysfunction, sustained VT, and severe mitral regurgitation 5 years ago. He had a history of RFCA for VT storm performed 2 months ago. In that session, 2 clinical VTs were ablated at the lateral and anterolateral areas of the LV for the VT storm. Although multiple VTs were induced via electrophysiological study, the procedure had to be terminated because of unstable vital signs and nonspontaneous clinical VTs. Following treatment in the cardiac care unit, he was discharged without VT on electrocardiogram monitoring. However, he suffered defibrillation shock from the VT 1 month after discharge. Owing to an underlying resistance to antiarrhythmic agents, he was admitted to our hospital for catheter ablation.

The workflow of the procedure was as follows. First, VT was induced to confirm whether the VT was bundle branch reentrant VT using electrophysiological study. Second, a voltage map of the LV was created, and pace mapping was performed to confirm which abnormal electrograms were related to the VT circuit, following the tagging of the

abnormal electrograms. Third, the coherent map confirmed that the slow conduction area matched the areas where clinical VTs were observed in the pace map. Fourth, ablation of the VT circuit was performed.

Electroanatomical mapping was done during the right ventricle (RV) pacing owing to the patient being pacing-dependent. Electroanatomical mapping using a multipolar mapping catheter (DECANAV catheter; Biosense Webster Inc, Diamond Bar, CA) revealed that multiple abnormal electrograms were widely spread in the LV, especially at the anterior, septum, apical, and inferior areas (Figure 1A). VTs were easily induced by right ventricular extrastimulus. Additionally, 3 VTs were induced (Figure 1B). Although mechanism of VT 1 was obscure owing to the ready switch to VT 2 or VT 3, it appeared to be reentry, because VT 1 was reproducibly induced by RV double extra pacing (S1–S1: 600 ms, S1–S2: 300 ms, and S2–S3: 300 ms). On the other hand, the mechanism of VT 2 was determined to have been owing to reentry, because of the constant fusion with the RV pacing observed during VT 2. Further electrophysiological study could not be performed owing to decreasing blood pressure, and thus an activation map could not be created during the arrhythmia. Moreover, because the abnormal electrograms were widely spread, it was difficult to differentiate which abnormal potential was related to the clinical VT circuit. Although time-consuming, the electrophysiological study demonstrated abnormal electrograms where the superoanterior (site A), inferobasal (site B), and inferoapical (site C) areas were closely related to these VT circuits (Figure 2). Figure 2 shows the coherent map integrated with voltage and vector map (CARTO®3 version 7; Biosense Webster). As shown in this figure, low-voltage areas were widely spread in the LV. However, slow conduction areas represented with bold arrows were located in the aforementioned areas—the superoanterior (site A; Figure 2A), inferobasal (site B; Figure 2B), and inferoapical areas (site C; Figure 2B). The pace map of sites A and B revealed a perfect pace map of VT 1 (Figure 3A) and VT 2 (Figure 3B). Furthermore, the stimulus-QRS were 34 ms and 50 ms, besides the tachycardia cycle lengths of 394 ms and 403 ms; thus, VT 1 and VT 2

were unable to be induced following RFCA at these areas. Figure 3C shows surface and intracardiac electrograms, which reveal concealed entrainment during pacing at site C during VT 3. In addition, the postpacing interval matched the tachycardia cycle length, and the stimulus-QRS matched the local potential-QRS. Figure 3D shows the ablation point. As shown in this figure, ablation points were located within the slow conduction area, which was represented by the coherent map integrated with a vector map. After final ablation for VT 3, any VTs could not be induced. During the 3-month follow-up, VT was not detected even in the device follow-up.

Written informed consent was obtained from the patient.

Discussion

In this case report, we describe a patient with multiple VTs where the critical isthmuses were located in the superoanterior, inferobasal, and inferoapical areas in the LV. Although locating the critical isthmuses was difficult owing to the widely spread abnormal electrograms, those that were clarified by the electrophysiological study and slow conduction areas using a coherent map integrated with a vector map were matched. RFCA for these areas eradicated the VTs.

RFCA decreases VT recurrence compared to medical therapy alone.[3] In addition, successful VT ablation improved not only the arrhythmia control, but also the transplant-free survival.[5] However, the recurrence rate was high at 30%–39%.[3,4] One of the mechanisms causing VT recurrence is the existence of multiple VT circuits owing to large scar areas.[5] In cases with large scar areas in the ventricle, it is difficult to differentiate which abnormal potentials are related to the critical VT circuit among the widely spread abnormal electrograms. Thus, in our case, despite the prior ablation performed for the VT storm, VT had not been eradicated owing to the multiple VT circuits present, secondary to the widespread abnormal potentials in our case.

Anter and colleagues[6] reported that the coherent mapping module enables one to more clearly describe complex propagation in an added vector map compared to the conventional mapping module in supraventricular tachycardia. In the coherent mapping module, the algorithm assigns each triangle on the reconstructed mesh with 3 descriptors: local activation time, conduction vector, and the probability of nonconductivity. Conduction velocities are calculated using the local activation time value and the known distance and direction between triangles.[6] Under these mechanisms, slow conduction areas are represented as bold arrows and normal conduction areas are represented as narrow arrows in vector maps that take into account global chamber propagation. Aziz and colleagues[7] reported that the isochronal late activation map can identify the functional substrate for VT. In that mapping, the area that is closely related to the VT circuit exhibited the greatest degree of conduction slowing. In the coherent map integrated with a vector map, this greatest degree of conduction slowing area may be represented with a bold arrow. In addition, the sudden change in local activation
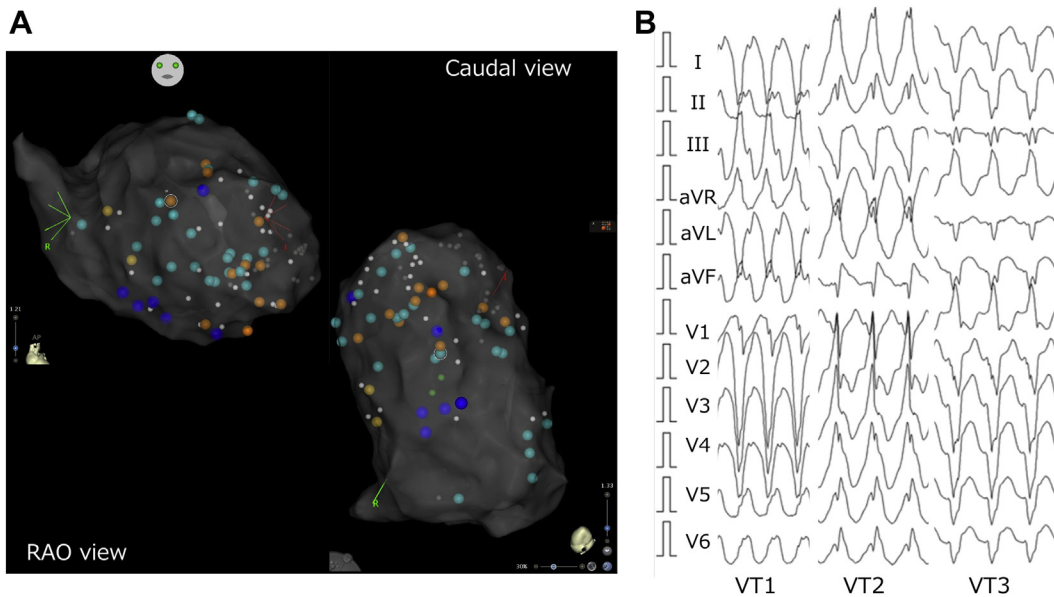
Figure 1 Three-dimensional mapping image and ventricular tachycardia (VT) morphologies on surface 12-lead electrocardiogram. **A:** The abnormal potentials in right anterior oblique (RAO) and caudal views of the left ventricle. Blue tag indicates isolated delayed potential, sky blue tag indicates isolated very delayed potential, and orange tag indicates local abnormal ventricular activity. **B:** Three VT morphologies on a surface 12-lead electrocardiogram.

time is not reflected by taking consistency among adjacent local activation time.[6] Therefore, we speculated that the dead-end pathway, which is within the VT circuit but is not related to the critical isthmus, may be excluded. In our case, although the abnormal electrograms were widely spread, slow conduction areas related to the VT circuit using a coherent map integrated with a vector map were matched using electrophysiological study. Therefore, a coherent map integrated with a vector map may clarify the critical

VT circuit. Additionally, the results of pace mapping at the slow conduction area in the coherent map integrated with a vector map indicated that the slow conduction area was the exit site of VT. We may have been able to explain the slow conduction area of the central isthmus if we had used a narrower interelectrode catheter as the mapping catheter. However, the VT activation map was not able to be created owing to decreasing blood pressure during VT. Adding the activation map during VT and comparing the activation
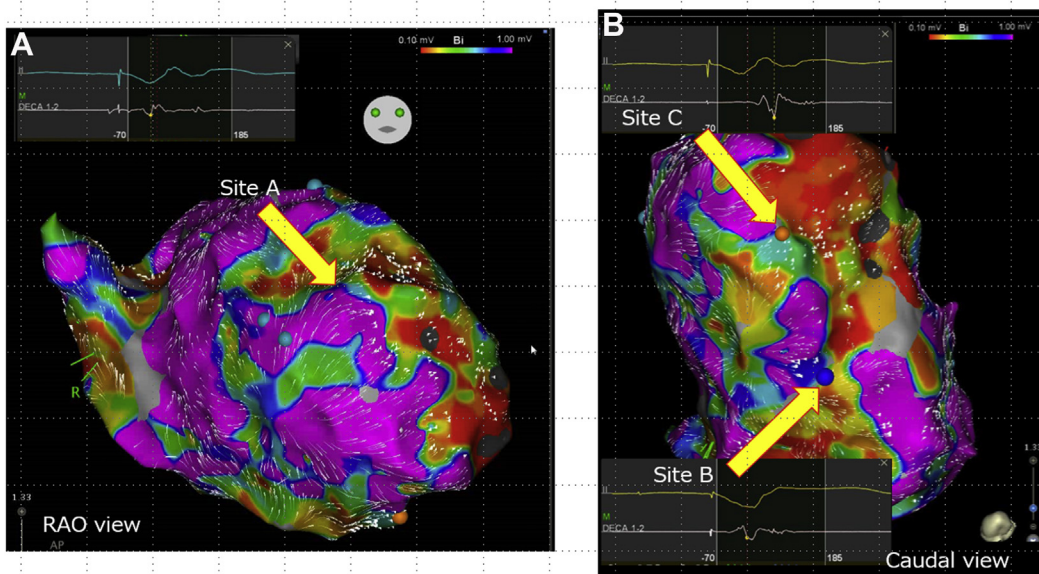

Figure 2 Coherent map integrated with voltage and vector map. **A:** Slow conduction area was observed (*arrow*) in the right anterior oblique (RAO) view. An isolated delayed potential was observed at site A. **B:** Slow conduction areas were observed in the caudal view, and isolated delayed potentials were observed at sites B and C (*arrows*). The bipolar voltage map settings were as follow: scar area was defined as less than 0.10 mV, low voltage area was defined as 0.10 to 1.00 mV, and the normal voltage area was defined as over 1.0 mV.
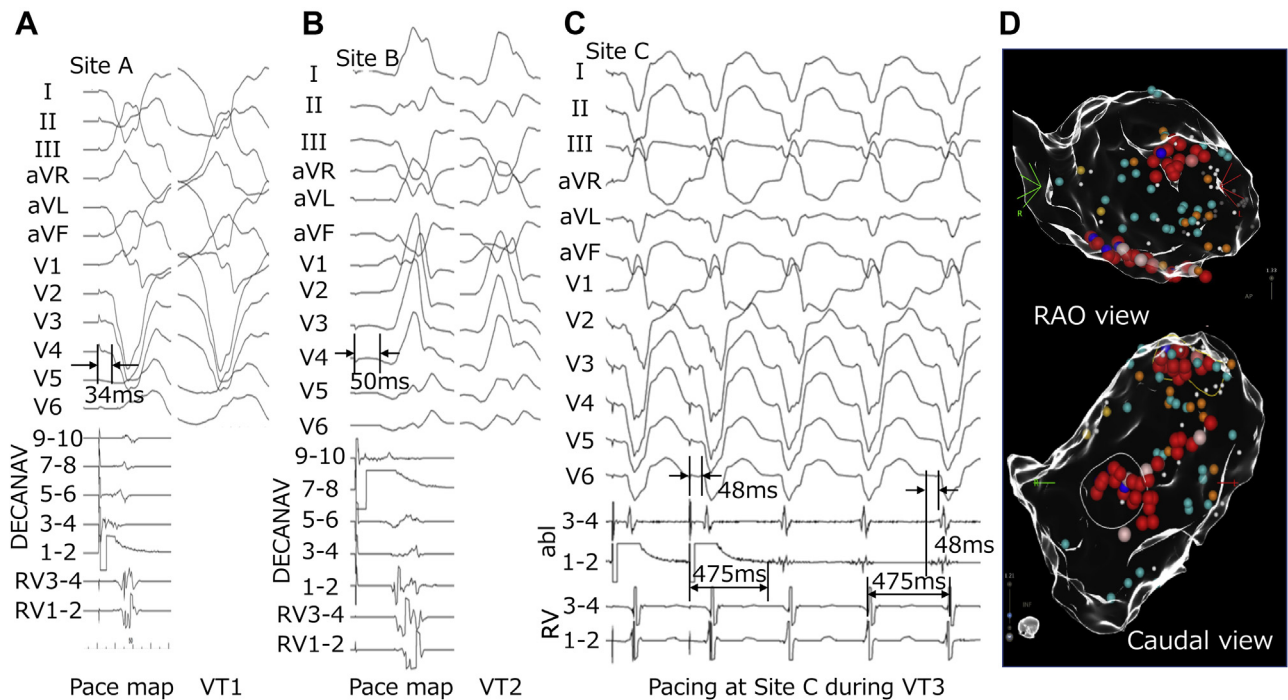
Figure 3   Each ventricular tachycardia (VT) morphology, electrophysiological study, and ablation point. **A, B:** The left sections show morphologies of surface 12-lead electrograms and local intracardiac electrograms during pace mapping at sites A and B, respectively. The right sections show VT 1 and VT 2 morphologies, respectively, on surface 12-lead electrograms. **C:** Twelve-lead electrograms and local intracardiac electrograms during entrainment pacing at site C during VT 3. **D:** Ablation points in right anterior oblique (RAO) view (top image) and in caudal view (bottom image). Red tags indicate ablation points.

map in the sinus or ventricular pacing may reveal the exact location of the slow conduction area among VT circuits, which should be considered in future studies.

With respect to the comparison between ripple mapping and coherent mapping, the ripple map was unable to clarify the critical VT circuit in our case initially. It has been reported that ripple mapping can help to reveal the VT substrate. However, voltage threshold adjustment is needed by individuals[8] because low voltage threshold not only represents abnormal electrograms but also exhibits noise, while high voltage threshold conceals abnormal electrograms, which may be related to the VT circuit. In fact, ripple mapping clarified the VT circuit only after adjusting the voltage threshold, following the confirmation of the slow conduction zone using coherent map integrated with a vector map. Therefore, to clarify the VT circuit using a ripple map, slow conduction zone must be confirmed first by the coherent map integrated with a vector map. Then, readjusting the voltage threshold may be a useful strategy.

In this case, we developed an ablation strategy through experience. First, we confirm the location of slow conduction areas in scar or border zones of the low voltage areas in coherent map integrated with a vector map. Second, we confirm whether there was an abnormal potential in these areas. Third, we proceed with ablation of the VT circuit following checking whether a pace map of these areas matched the VT morphology.

Conclusion

A coherent map integrated with a vector map may enable us to differentiate which abnormal potential is related to the critical slow conduction area, even in multiple and complex VT cases, like the one presented herein. A coherent map integrated with a vector map may be useful to identify the critical VT target, especially in cases where the VT has multiple critical circuits.

Acknowledgments

The authors would like to thank Mr Shogo Tsuda and Mr Taiki Harada.

References

1. Al-Khatib SM, Stevenson WG, Ackerman MJ, et al. 2017 AHA/ACC/HRS guideline for management of patients with ventricular arrhythmias and the prevention of sudden cardiac death: Executive summary: A report of the American College of Cardiology/American Heart Association task force on clinical practice guidelines and the Heart Rhythm Society. Circulation 2018;138:e210–e271.
2. Priori SG, Blomström-Lundqvist C, Mazzanti A, et al. 2015 ESC guidelines for the management of patients with ventricular arrhythmias and the prevention of sudden cardiac death: The task force for the management of patients with ventricular arrhythmias and the prevention of sudden cardiac death of the European Society of Cardiology (ESC). Endorsed by: Association for European Paediatric and Congenital Cardiology (AEPC). Eur Heart J 2015;36:2793–2867.
3. Anderson RD, Ariyarathna N, Lee G, et al. Catheter ablation versus medical therapy for treatment of ventricular tachycardia associated with structural heart disease: systematic review and meta-analysis of randomized controlled trials and comparison with observational studies. Heart Rhythm 2019;16:1484–1491.
4. De Silva K, Virk S, Nalliah CJ, Campbell T, Kumar S. Multielectrode mapping versus point-by-point mapping for catheter ablation of ventricular tachycardia: a systematic review and meta-analysis. JACC Clin Electrophysiol 2020;6:876–878.

5. Tung R, Vaseghi M, Frankel DS, et al. Freedom from recurrent ventricular tachy-cardia after catheter ablation is associated with improved survival in patients with structural heart disease: an international VT ablation center collaborative group study. Heart Rhythm 2015;12:1997–2007.
6. Anter E, Duytschaever M, Shen C, et al. Activation mapping with integration of vector and velocity information improves the ability to identify the mechanism and location of complex scar-related atrial tachycardias. Circ Arrhythm Electrophysiol 2018;11:e006536.
7. Aziz Z, Shatz D, Raiman M, et al. Targeted ablation of ventricular tachycardia guided by wavefront discontinuities during sinus rhythm: a new functional substrate mapping strategy. Circulation 2019; 140:1383–1397.
8. Jamil-Copley S, Vergara P, Carbucicchio C, et al. Application of ripple mapping to visualize slow conduction channels within the infarct-related left ventricular scar. Circ Arrhythm Electrophysiol 2015;8:76–86.